

Supporting Information for

Co(cyclam) Complexes of Triarylamine-acetylide: Structural and Spectroscopic Properties and DFT analysis

Susannah D. Banziger, Adharsh Raghavan, Matthias Zeller and Tong Ren

Department of Chemistry, Purdue University, West Lafayette, Indiana 47906, USA

Table of Contents:

1. Crystallographic Details S2-S5
2. Normalized absorption and emission spectra S6
3. Gaussian fit peak analysis for transitions between 20,000 cm⁻¹ and 8,000 cm⁻¹ S7
4. ¹H NMR Spectra [**1**]Cl, **2a**, **2b**, and [**3**]Cl S8-S9
5. Computational details S10-S23

Single Crystal X-ray Structure Analyses

X-ray diffraction data for [1]Cl, **2a**, **2b** and [3]Cl were obtained on a Bruker Quest diffractometer with a Photon100 CMOS area detector, a fixed chi angle, a sealed tube fine focus X-ray tube, and a single crystal curved graphite incident beam monochromator. Data were collected with MoK α radiation ($\lambda = 0.71073$ Å) at 150K. Data were collected; reflections were indexed and processed using APEX3. The space groups were assigned and the structures were solved by direct methods using XPREP within the SHELXTL suite of programs¹ and refined using Shelxl and Shelxle.

If not specified otherwise H atoms attached to carbon, boron and nitrogen atoms as well as hydroxyl hydrogens were positioned geometrically and constrained to ride on their parent atoms. C-H bond distances were constrained to 0.95 Å for aromatic and alkene C-H and CH₂ moieties, and to 0.99 and 0.98 Å for aliphatic CH₂ and CH₃ moieties, respectively. N-H bond distances were constrained to 1.00 Å for pyramidal (sp³ hybridized) ammonium NH⁺ groups. O-H distances of alcohols were constrained to 0.84 Å. Methyl CH₃ hydroxyl H atoms were allowed to rotate but not to tip to best fit the experimental electron density. U_{iso}(H) values were set to a multiple of U_{eq}(C) with 1.5 for CH₃ and OH, and 1.2 for C-H, CH₂ and N-H units, respectively.

Additional crystallographic data for [1]Cl, **2a**, **2b** and [3]Cl are provided below and in Table S1.

CCDC 2013775-2013778 contain the supplementary crystallographic data for compounds [1]Cl, **2a**, **2b** and [3]Cl respectively. These data can be obtained free of charge from The Cambridge Crystallographic Data Centre.

Table S1. Crystal data for complexes [1]Cl, 2a, 2b and [3]Cl

	[1]Cl·THF·CH ₃ OH	2a·THF	2b·CH ₃ OH	[3]Cl·CH ₂ Cl ₂
Chemical Formula	C ₃₂ H ₄₂ ClCoN ₅ O ₂ ·0.247(C ₄ H ₁₀ O)·1.507(CH ₄ O)·0.05(I)·0.95(Cl)	C ₃₂ H ₄₂ Cl ₃ CoCuN ₅ O ₂ ·C ₄ H ₈ O	C ₃₂ H ₄₂ AgCoN ₈ O ₁₁ ·1.476(CH ₄ O)·0.209(O)	C ₅₄ H ₆₀ CoN ₆ O ₄ ·0.874(CH ₂ Cl ₂)·0.415(Br)·0.585(Cl)
Formula Weight	729.67	829.63	933.70	1044.11
Space Group	Monoclinic, <i>P</i> ₂ ₁ / <i>c</i>	Triclinic, <i>P</i> $\bar{1}$	Triclinic, <i>P</i> $\bar{1}$	Triclinic, <i>P</i> $\bar{1}$
<i>a</i> , Å	14.2721 (8)	9.3921 (8)	10.5925 (6)	11.8848 (12)
<i>b</i> , Å	24.1352 (13)	13.371 (2)	11.7280 (7)	13.9746 (18)
<i>c</i> , Å	10.4474 (5)	15.203 (2)	16.0527 (9)	15.972 (3)
α , deg	-	86.645 (3)	93.730 (2)	104.155 (6)
β , deg	93.064 (2)	77.678 (4)	98.254 (2)	91.216 (6)
γ , deg	-	85.353 (3)	96.435 (2)	91.053 (4)
<i>V</i> , Å ³	3593.6 (3)	1857.4 (4)	1954.4 (2)	2570.8 (6)
<i>Z</i>	4	2	2	2
<i>T</i> , K	150	150	150	150
λ , Å	0.71073	0.71073	0.71073	0.71073
$\Delta\rho_{\max}$, $\Delta\rho_{\min}$ (e Å ⁻³)	0.66, -0.39	0.42, -0.47	1.15, -1.12	0.72, -0.39
<i>R</i>	0.046	0.026	0.041	0.044
<i>R</i> _w (<i>F</i> ²)	0.126	0.085	0.103	0.142

Special Refinement Details

The O4 methanol is partially substituted by an ether molecule. This affects the hydrogen bonding of the O3 molecule, extending the disorder to it. The U^{ij} components of the ADPs for all disordered atoms within 2.0 Å were restrained to be similar. The distances from oxygen to the first and second carbon on the ether molecule were restrained to be similar to the opposing side. Each C--C distance on ether was also restrained to 1.53(2) Å. Further DFIX commands were used for hydrogen bonding considerations. Subject to these conditions, the occupancy for the A and B labelled methanol atoms refined to 0.507(6) and 0.493(6), respectively. The ether molecule is located on an inversion center and its occupancy refines to exactly one half of the B labelled methanol with a value of 0.247(3). The chloride anion is partially displaced by an iodide impurity, refining with occupancies of 0.950(2) and 0.050(2), respectively.

Compound 2a

The tetrahydrofuran solvent molecule was refined as two disordered moieties. The B moiety was restrained to have a similar geometry to the A moiety. All atoms within 2.0 Å were restrained to have similar U^{ij} components. Subject to these conditions, the occupancy factors for the A and B moieties refined to 0.729(5) and 0.271(5), respectively.

Compound 2b

Disorder of an anisyl ring is correlated with solvent methanol molecule disorder. The anisyl ring (C16-O2B) refined as two separate moieties with the methyl groups pointing in opposite directions. The two moieties were restrained to have similar geometries (SAME command of SHELXL) and U^{ij} components of ADPs for disordered atoms closer to each other than 2.0 Å were restrained to be similar. Subject to these conditions the occupancy refined to 0.585(6) for C16-O2 and 0.414(4) for C16B-O2B. Correlated to the anisyl disorder is disorder of several methanol molecules. They were refined as four disordered moieties, of which the U^{ij} components of ADPs were all restrained to be similar for atoms closer to each other than 2.0 Å. All methanol O-C bond distances were restrained to 1.45(2) Å. O13 is a partially occupied water molecule disordered with one of the anisyl methoxy groups and refined to 0.209(4) occupancy. Hydrogen atoms were omitted for this partially occupied water molecule. For the two methanol moieties closest to the major methoxy moiety the sums of occupancies were restrained to unity. For all other methanol and water moieties full occupancy was not enforced. Positions of methanol hydroxyl H atoms were initially restrained based on hydrogen bonding considerations (DFIX commands restraining the distance to the acceptor atom). In the final refinement cycles they were set to ride on their carrier oxygen atoms. One of the nitrates directly attached to Ag refined as two disordered moieties and were restrained to be similar. The two moieties were restrained to have similar geometries (SAME command of SHELXL) and U^{ij} components of ADPs for disordered atoms closer to each other than 2.0 Å were restrained to be similar. Subject to these conditions occupancies refined to 0.49(3) and 0.51(3).

Compound [3]Cl

The anion site is shared between chloride and bromide. Positions and ADPs of Cl1 and Br1 were constrained to be identical, leading to a refined occupancy ratio of 0.585(2) to 0.415(2) in favor of chloride. A solvate pocket is occupied by disordered methylene chloride molecules. The moieties were restrained to have similar geometries with similar C-Cl distances, and U^{ij} components of ADPs were restrained to be similar for atoms closer to each other than 1.7 Å. Subject to these conditions the occupancy rates refined to 0.416(7), 0.289(4), 0.079(3) and 0.090(6).

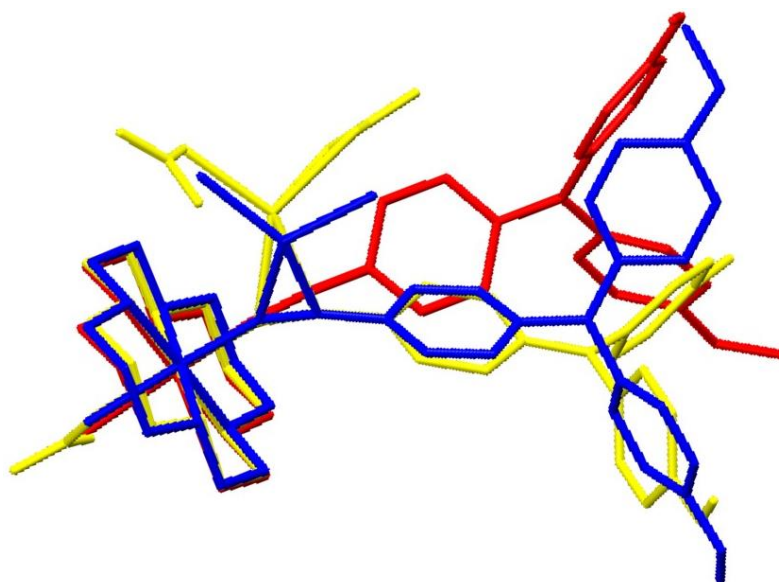


Figure S1. Overlay of compounds **[1]Cl** (red), **2a** (blue) and **2b** (yellow) showing the effect of η^2 coordination on the Co-C1-C2-C3 dihedral angle.

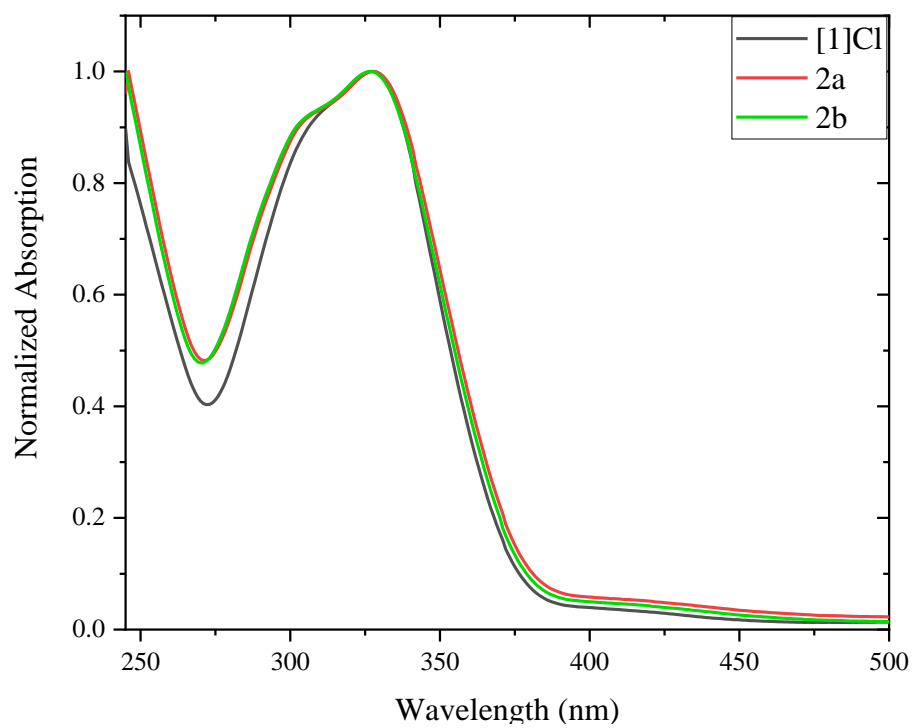


Figure S2. Normalized absorption spectra of [1]Cl, 2a and 2b in CH_2Cl_2

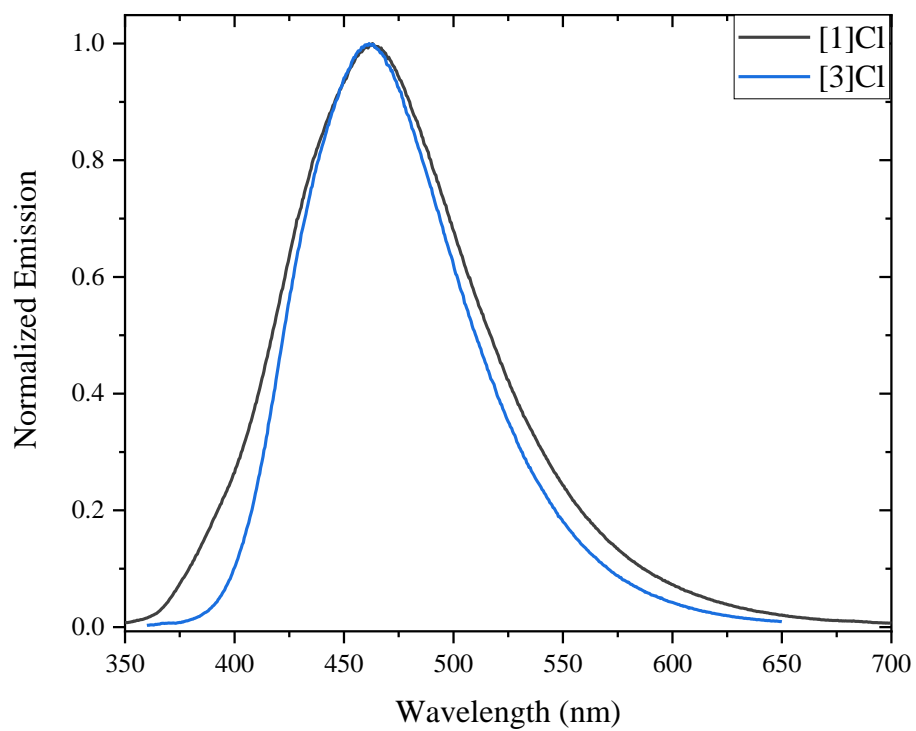


Figure S3. Normalized emission spectra of [1]Cl and [3]Cl in CH_2Cl_2 at room temperature

Table S2. Gaussian fit peak analysis for transitions between 20,000 cm^{-1} (500 nm) and 8,000 cm^{-1} (1250 nm). The deconvoluted spectra are shown in Figure S4 and Figure S5.

Compound	Peak	^a E _{OP} (cm^{-1})	^a ϵ_{max} ($\text{M}^{-1}\text{cm}^{-1}$)	^b $\Delta\nu_{1/2}$ (cm^{-1})	^c r (Å)
[1]Cl	A	14003	5928	2928	8.757
[1]Cl	B	12030	6028	1655	8.757
[3]Cl	A	15158	19105	2475	8.848
[3]Cl	B	13277	25244	2119	8.848
[3]Cl	C	11273	19105	1499	8.848

^aMeasured by spectroelectrochemical oxidation. ^bDetermined from deconvoluted spectral analysis ($\Delta\nu_{1/2}$ = fwhm).

^cDetermined based on the geometric distance between the Co^{III} metal center and the nitrogen atom of the TPA group in the collected crystal structures. See Figures S4 and S5 for specific assignment.

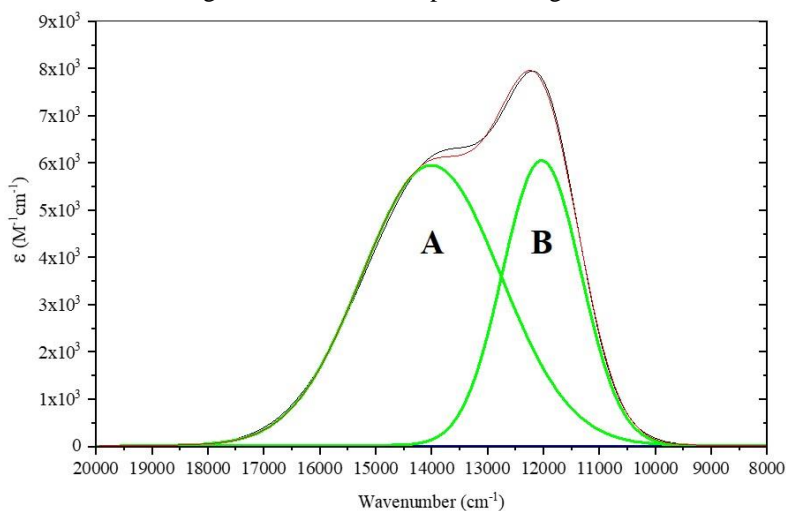


Figure S4. Deconvoluted spectra of the oxidation product from holding compound [1]Cl at 0.88 V in a MeCN solution containing 0.1 M *n*-Bu₄NPF₆.

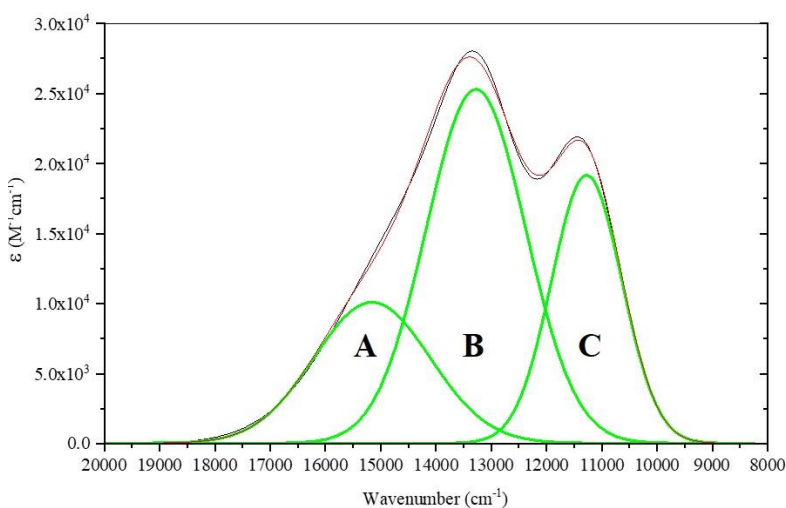


Figure S5. Deconvoluted spectra of the oxidation product formed from holding compound [3]Cl at 0.88 V in a MeCN solution containing 0.1 M *n*-Bu₄NPF₆.

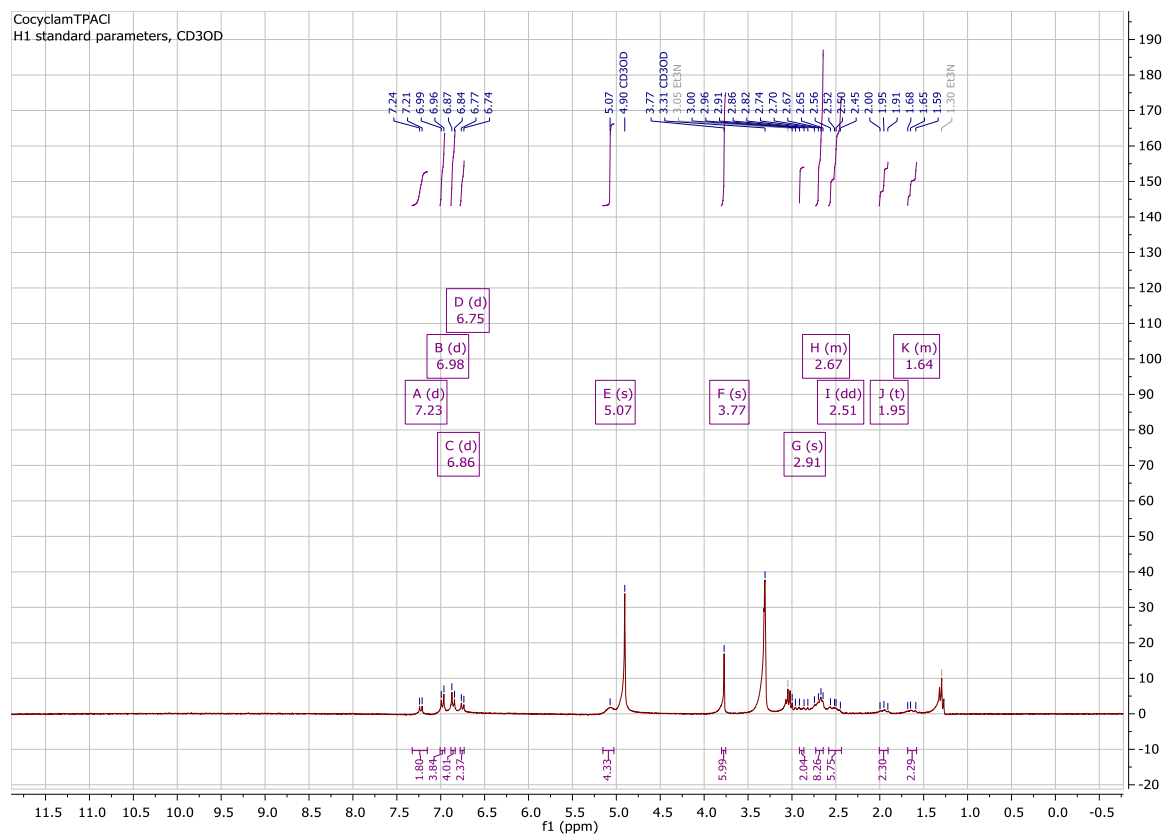


Figure S6. ^1H NMR of $[1]\text{Cl}$ $[\text{Co}(\text{cyclam})(\text{C}_2\text{TPA})\text{Cl}]\text{Cl}$ in CD_3OD

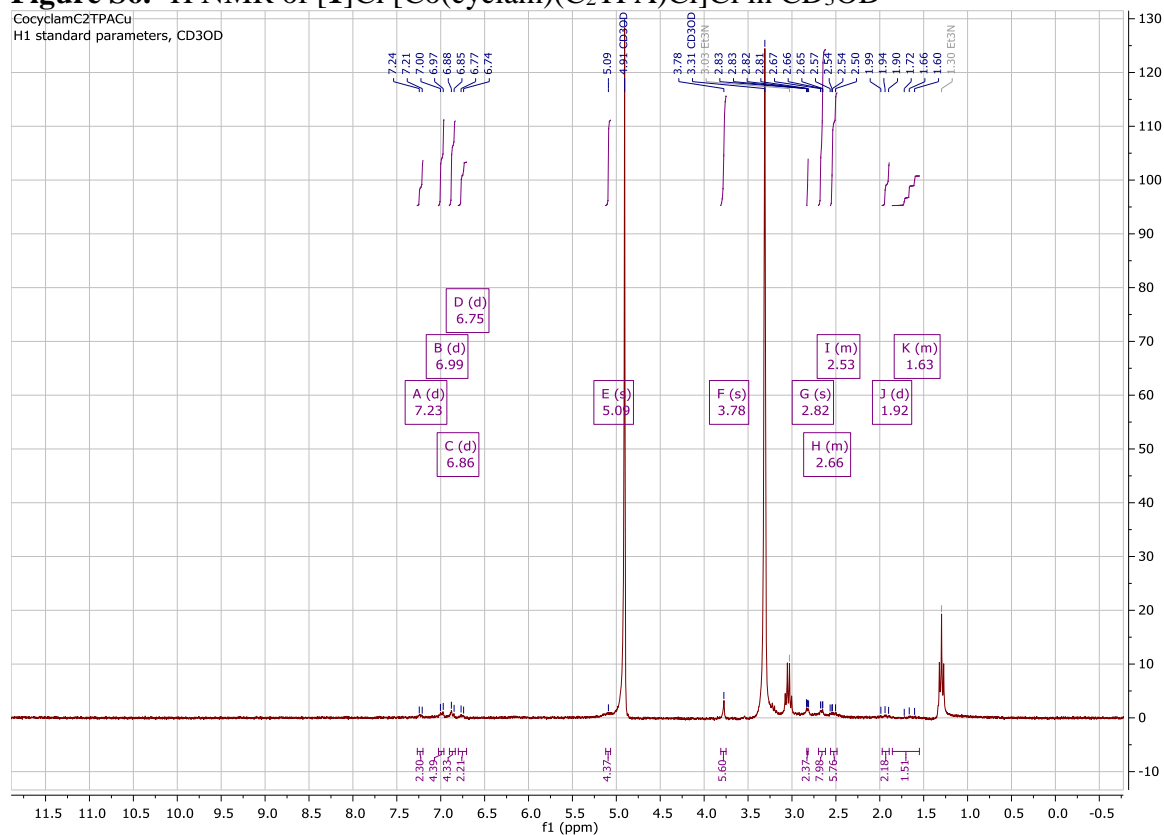


Figure S7. ^1H NMR of 2a $[\text{Co}(\text{cyclam})(\text{C}_2\text{TPA}-\eta^2\text{-CuCl}_2)\text{Cl}]$ in CD_3OD

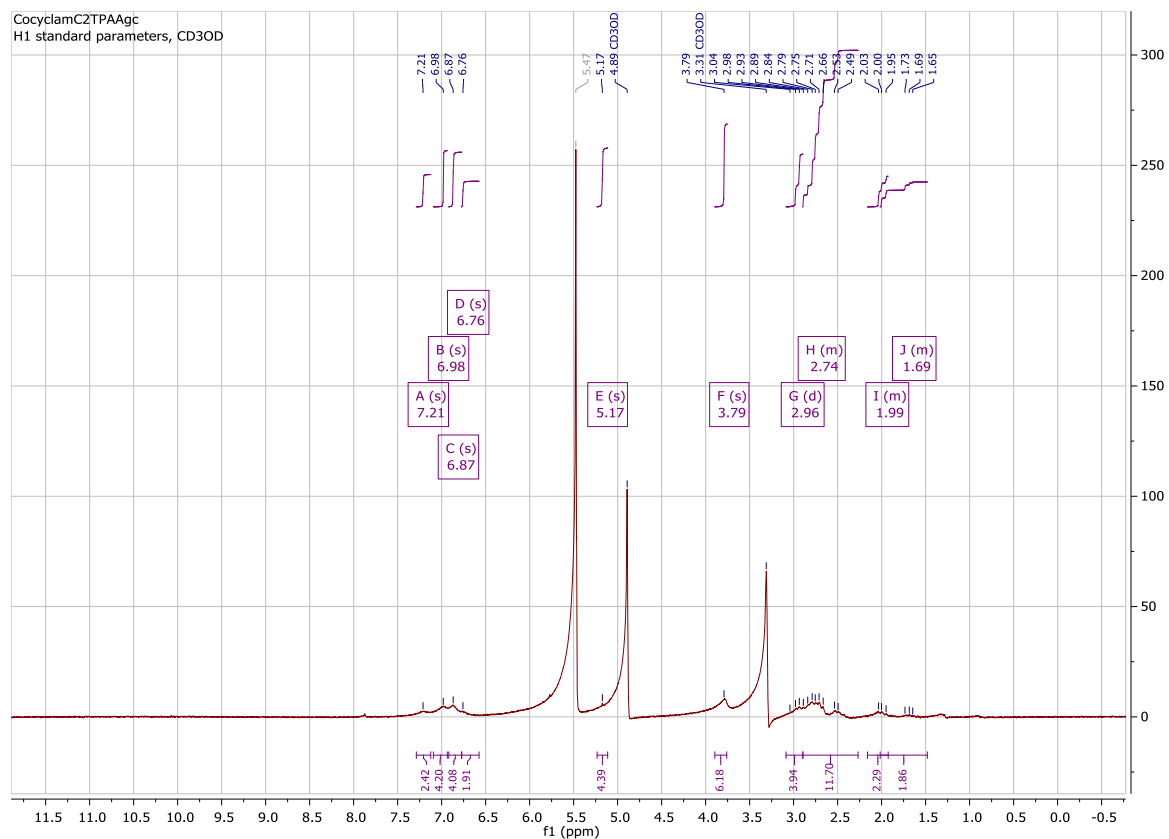


Figure S8. ^1H NMR of **2b** $[\text{Co}(\text{cyclam})(\text{C}_2\text{TPA}-\eta^2\text{-Ag}(\text{NO}_3)_2)(\text{NO}_3)]$ in CD_3OD



Figure S9. ^1H NMR of **[3]Cl** $[\text{Co}(\text{cyclam})(\text{C}_2\text{TPA})_2]\text{Cl}$ in CDCl_3

Computational details

All DFT calculations were performed using Gaussian16 (rev. A.03) program.² Both ground and excited state calculations were performed at the same level of theory. While the functionals B3LYP,³⁻⁶ BP86,⁵ CAM-B3LYP,⁷ M06,⁸ wB97X⁹ and M06HF.¹⁰ All gave ground-state metrical parameters close to experimentally obtained ones for [1]⁺ and [3]⁺, excited state calculations were more or less accurate only in the case of M06. Hence, all further calculations were carried out using this functional.

The def2-tzvp¹¹ basis set was used for Co and 6-31G(d,p)^{12,13} for all other atoms. Additionally, a solvation model (polarizable continuum model^{14,15} for acetonitrile) and Grimme's empirical dispersion correction parameters were employed for all calculations.¹⁶ For all ground-state calculations, minima were ensured through vibrational frequency analyses.

The M06-HF functional, which employs 100% HF exchange performed very poorly. Both B3LYP and the long-range-corrected functional CAM-B3LYP, which has been utilized previously for Fc-TPA systems¹⁷ also performed poorly. The M06 functional, which employs 27% HF exchange, was found to be the most accurate for these systems. The Tamm-Dancoff approximation (TDA) was used for all TD-DFT calculations since it is known to give results that are close to, or sometimes even better than full linear-response TD-DFT.¹⁸ In order to better visualize the qualitative nature of the electronic transitions, natural transition orbitals (NTOs) were computed using the method developed by Martin.¹⁹

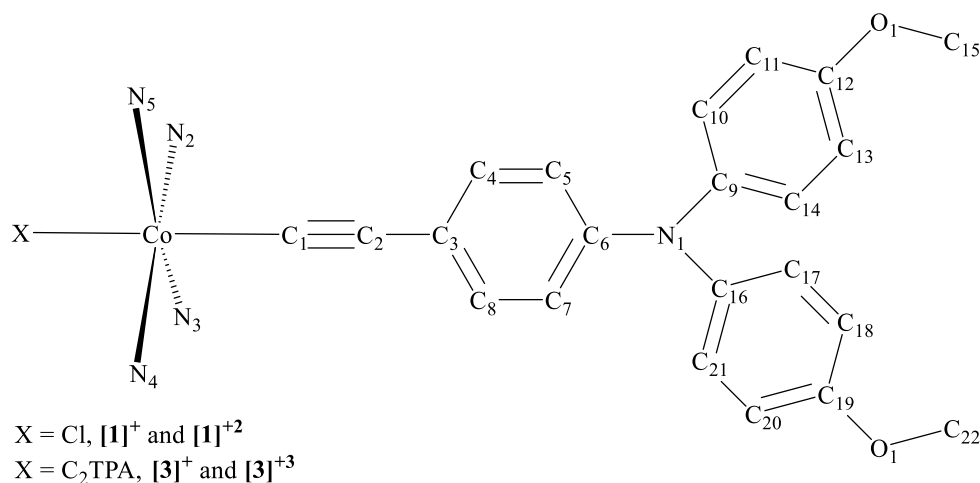


Chart S1. Schematic legend for Table S3

Table S3. Comparison of experimental and DFT-optimized metrical parameters^a

	[1] ⁺ , expt	[1] ⁺	[1] ⁺²	[3] ⁺ , expt	[3] ⁺	[3] ⁺³
Co–Cl	2.3401(7)	2.33104	2.32111	-	-	-
Co–N _{cyclam} (ave)	1.975[1]	1.99042	1.99095	1.990[1]	1.99457	1.99598
Co–C1	1.879(3)	1.88642	1.88356	1.945(2)	1.93688	1.92984
C1–C2	1.205(4)	1.22539	1.22610	1.203(3)	1.22859	1.22921

C2–C3	1.434(4)	1.42671	1.41871	1.446(3)	1.42731	1.41769
C3–C4	1.395(4)	1.40315	1.40743	1.402(3)	1.40465	1.40959
C4–C5	1.382(4)	1.38460	1.37973	1.388(3)	1.38435	1.37870
C5–C6	1.393(4)	1.40384	1.40509	1.407(3)	1.40370	1.40585
C6–C7	1.388(4)	1.40394	1.40527	1.406(3)	1.40305	1.40553
C7–C8	1.387(4)	1.38410	1.37904	1.388(3)	1.38527	1.37912
C8–C3	1.404(4)	1.40406	1.40888	1.405(3)	1.40347	1.40866
N1–C6	1.431(3)	1.40152	1.40414	1.410(3)	1.40290	1.40309
N1–C9	1.420(4)	1.42012	1.40276	1.434(3)	1.41988	1.40319
C9–C10	1.391(4)	1.39371	1.40353	1.381(4)	1.39374	1.40315
C10–C11	1.376(4)	1.39226	1.38181	1.401(4)	1.39239	1.38197
C11–C12	1.388(5)	1.39572	1.40339	1.365(4)	1.39574	1.40310
C12–C13	1.386(4)	1.39936	1.40696	1.398(4)	1.39933	1.40683
C13–C14	1.388(4)	1.38358	1.37430	1.385(4)	1.38359	1.37459
C14–C9	1.384(4)	1.39991	1.40859	1.383(4)	1.40004	1.40834
C12–O1	1.375(4)	1.35625	1.33638	1.371(3)	1.35653	1.33688
O1–C15	1.417(5)	1.41181	1.42085	1.435(4)	1.41176	1.42059
Co–C1–C2	172.6(2)	175.09752	176.6865	175.8(2)	174.77895	176.18823
C1–C2–C3	171.6(3)	178.37572	178.39047	177.5(3)	177.80433	177.59653

^a there is a mirror symmetry along Co – N₁ vector and bisecting the acetylene bearing phenyl group. Atoms related by this symmetry are omitted.

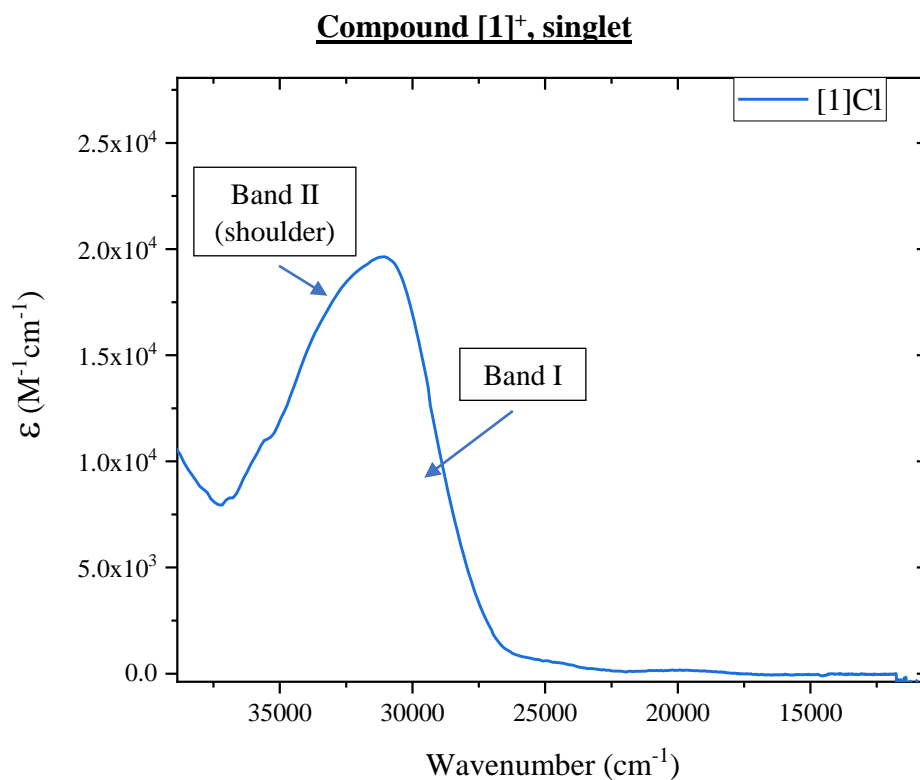


Figure S10. Experimental UV-Vis spectrum of [1]Cl in MeCN. The major peak (and its associated shoulder) in the spectrum can be split into two bands: I and II (shoulder).

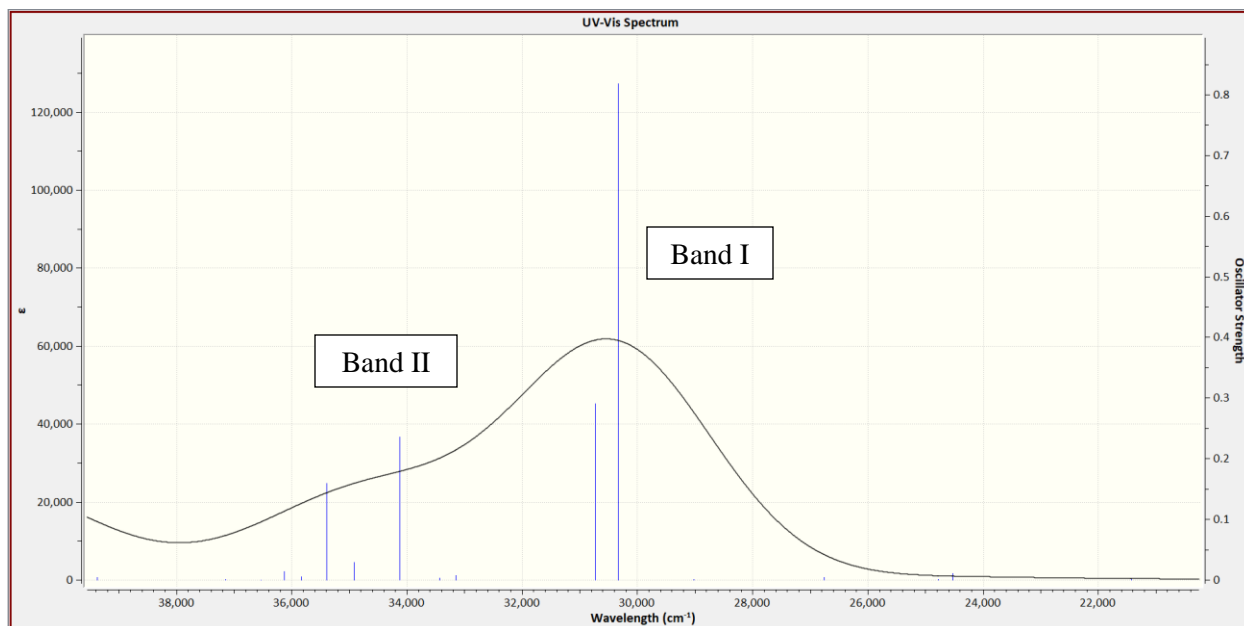
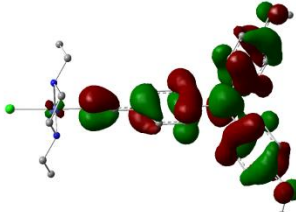
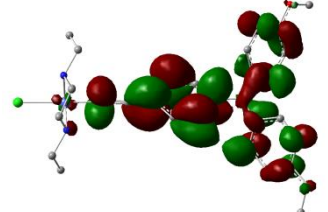
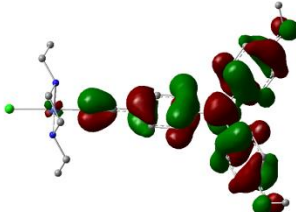
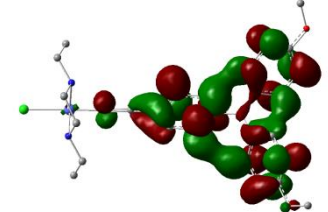
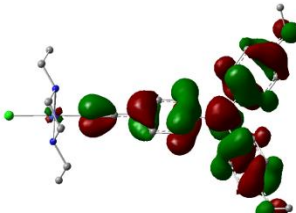
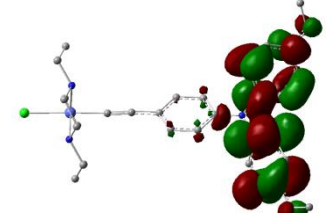
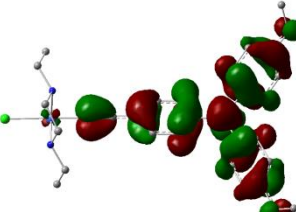
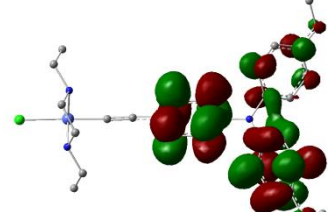


Figure S11. TD-DFT-simulated UV-Vis spectrum of [1]⁺

While there are noticeable quantitative differences between experiment and theory (molar absorptivities, especially), there is qualitative agreement on the existence of two major bands, each consisting of very few closely spaced transitions. TD-DFT over-estimates the energies of

the transitions associated with ‘Band II’. Bands I and II both consist of $\pi \rightarrow \pi^*$ transitions involving either the TPA moiety or the $\text{C}\equiv\text{C}$ -TPA moiety. The associated excited states and Natural Transition Orbitals (NTOs) are:

Table S4. NTOs computed for the excited states of $[\mathbf{1}]^+$. Transitions are noted in the direction NTO1 (hole) \rightarrow NTO2 (electron). |isovalue| = 0.025.

Excited state	$\bar{\nu}$ (cm^{-1})	Oscillator strength	NTO1	NTO2
S9	30330.6	0.8183		
S10	30729.5	0.2911		
S13	34129.7	0.2359		
S15	35390.7	0.1594		

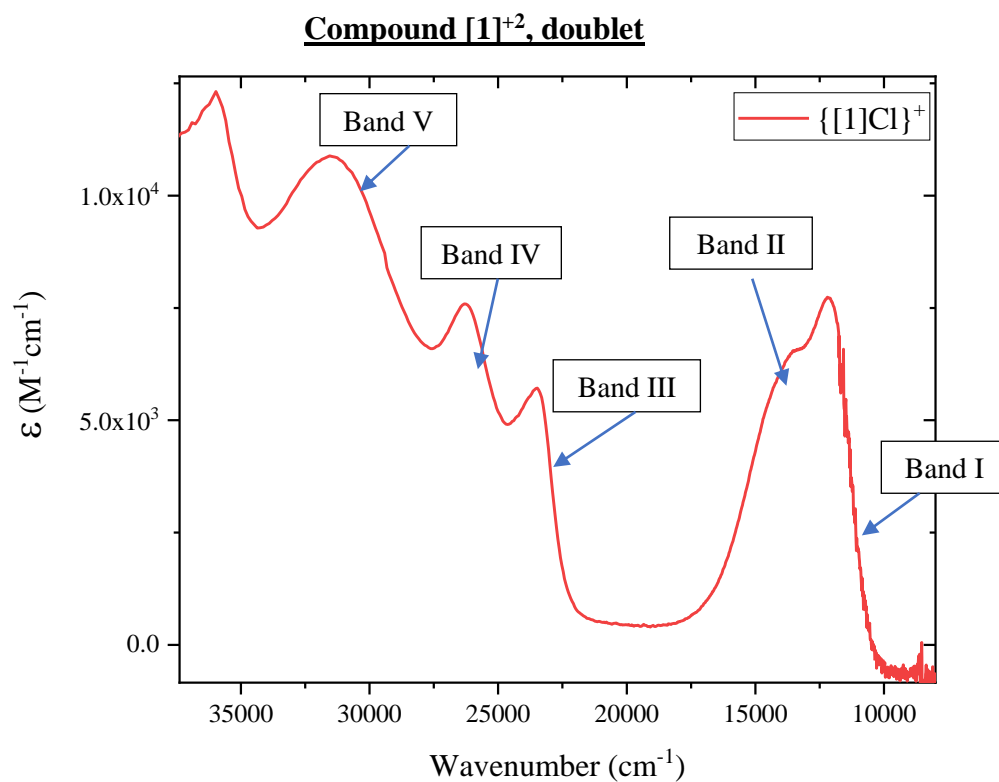


Figure S12. Experimental UV-Vis spectrum of {[1]Cl}⁺ in MeCN, obtained by spectroelectrochemistry.

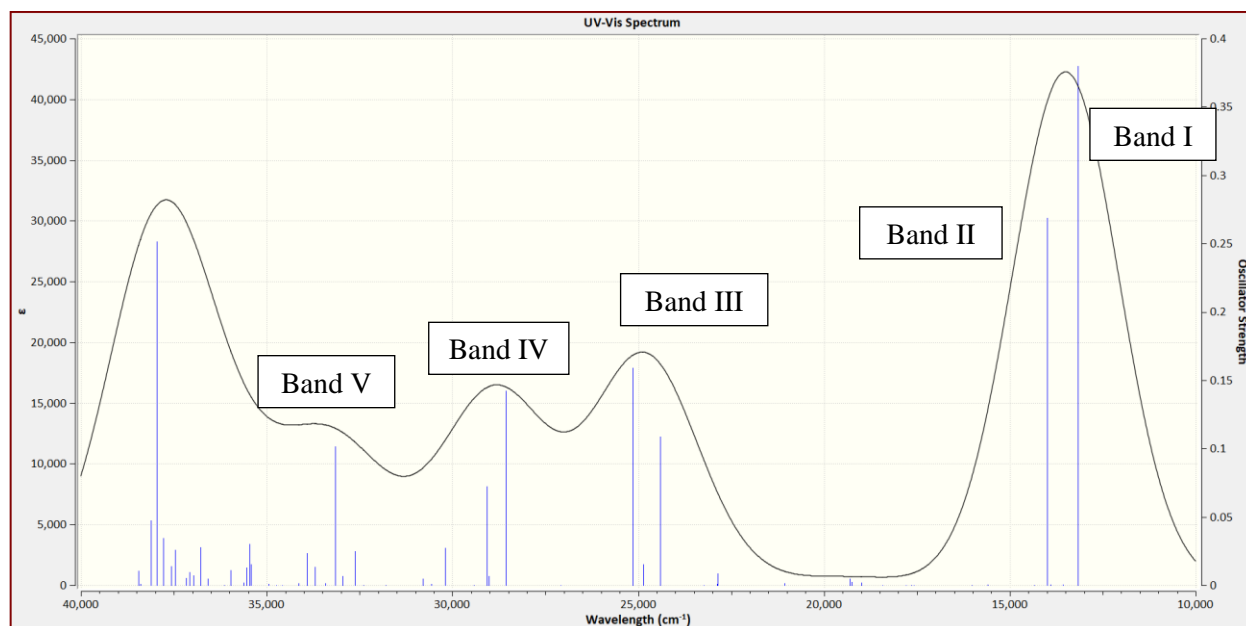
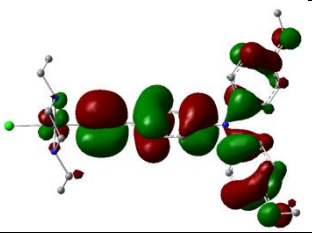
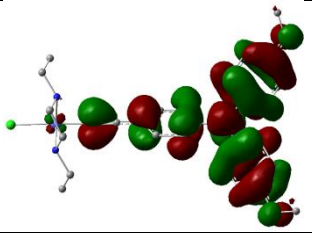
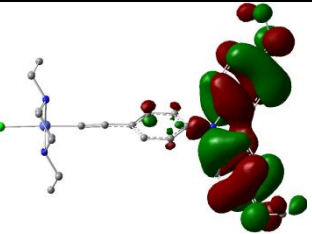
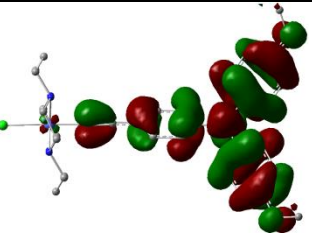
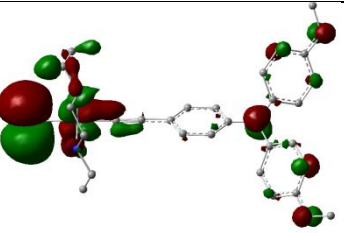
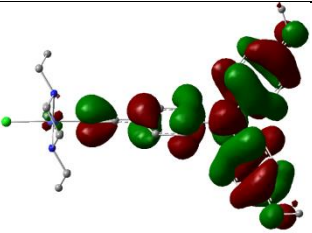
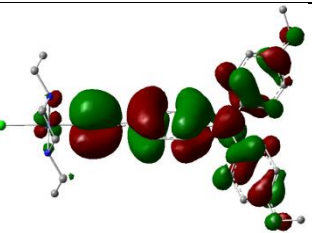
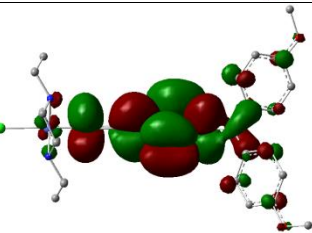
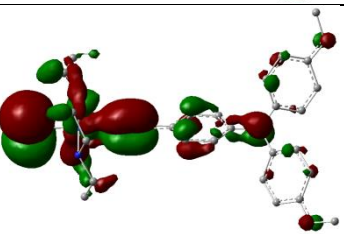
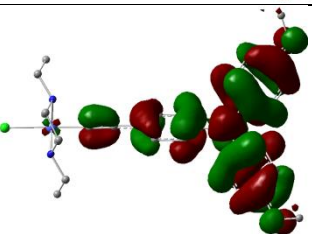
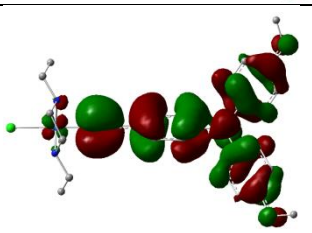
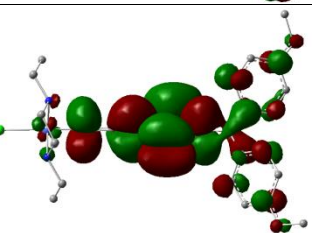
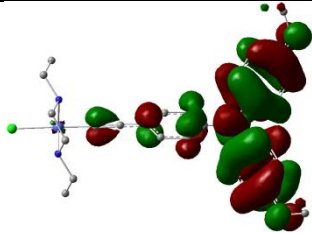
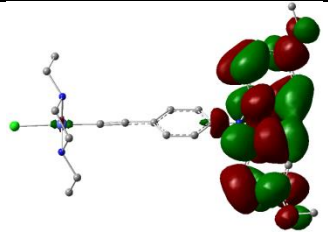
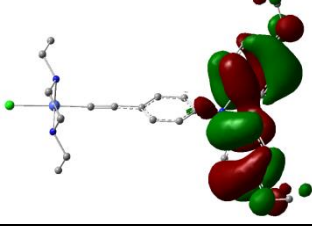
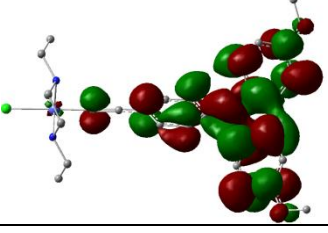
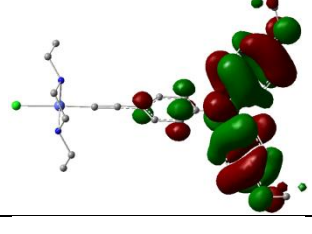
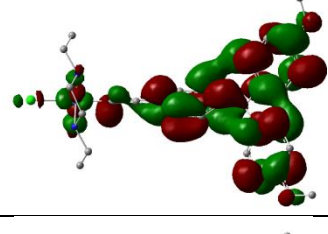
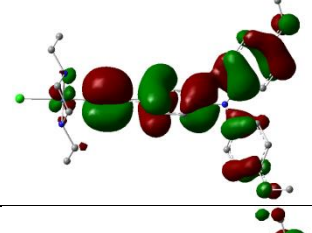
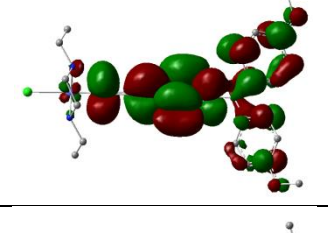
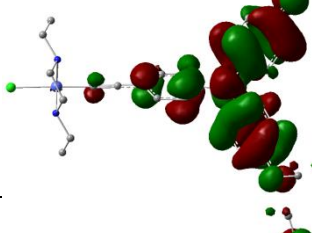
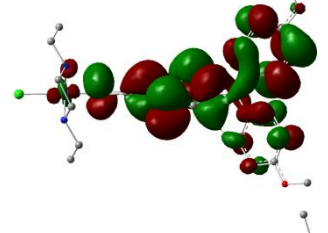
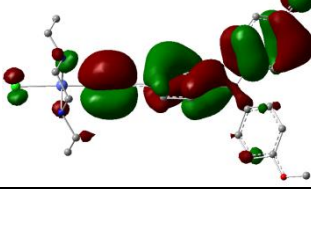
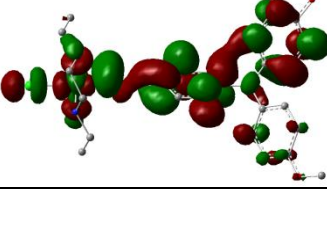


Figure S13. TD-DFT simulated UV-Vis spectrum of [1]⁺².

Table S5. NTOs computed for the excited states of $[1]^{+2}$. Transitions are noted as NTO1 (hole) \rightarrow NTO2 (electron). |isovalue| = 0.025.

Excited state	$\bar{\nu}$ (cm^{-1})	Oscillator strength	NTO1	NTO2
D1	13164.8	0.3797		
D4	13987.6	0.2686		
D19 major	24417	0.1087		
D19 minor	24417	0.1087		
D21 major	25145.2	0.159		
D21 minor	25145.2	0.159		

D23 major	28563.0	0.1422		
D23 minor	28563.0	0.1422		
D25 major	29080.7	0.0724		
D25 minor	29080.7	0.0724		
D34 major	33147.7	0.1014		
D34 major	33147.7	0.1014		

Compound [3]⁺, singlet

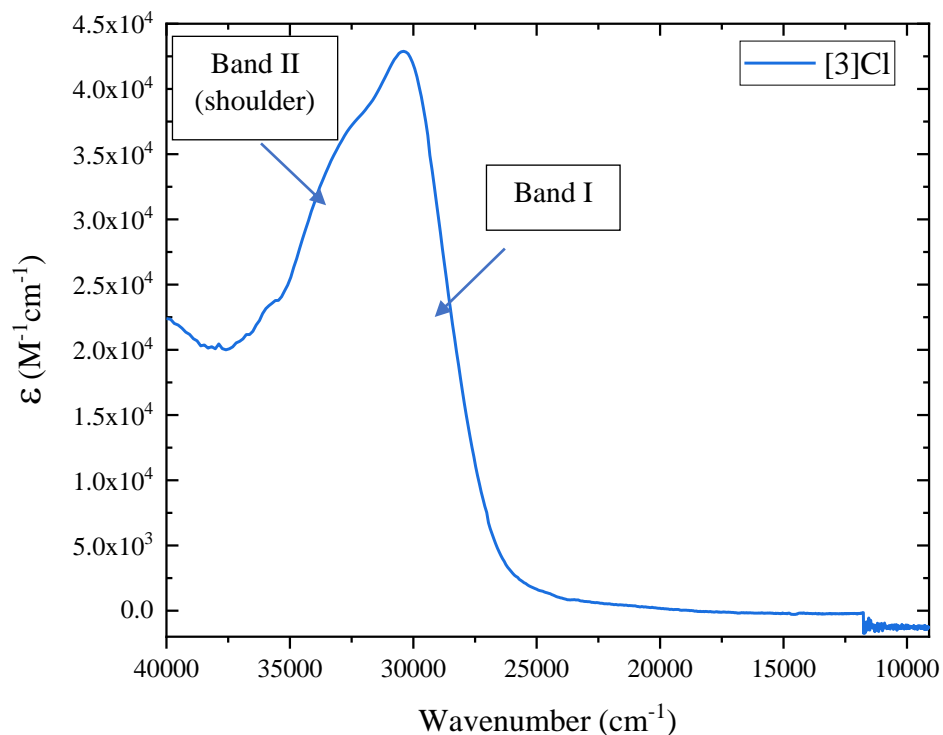


Figure S14. Experimental UV-Vis spectrum of [3]Cl in MeCN.

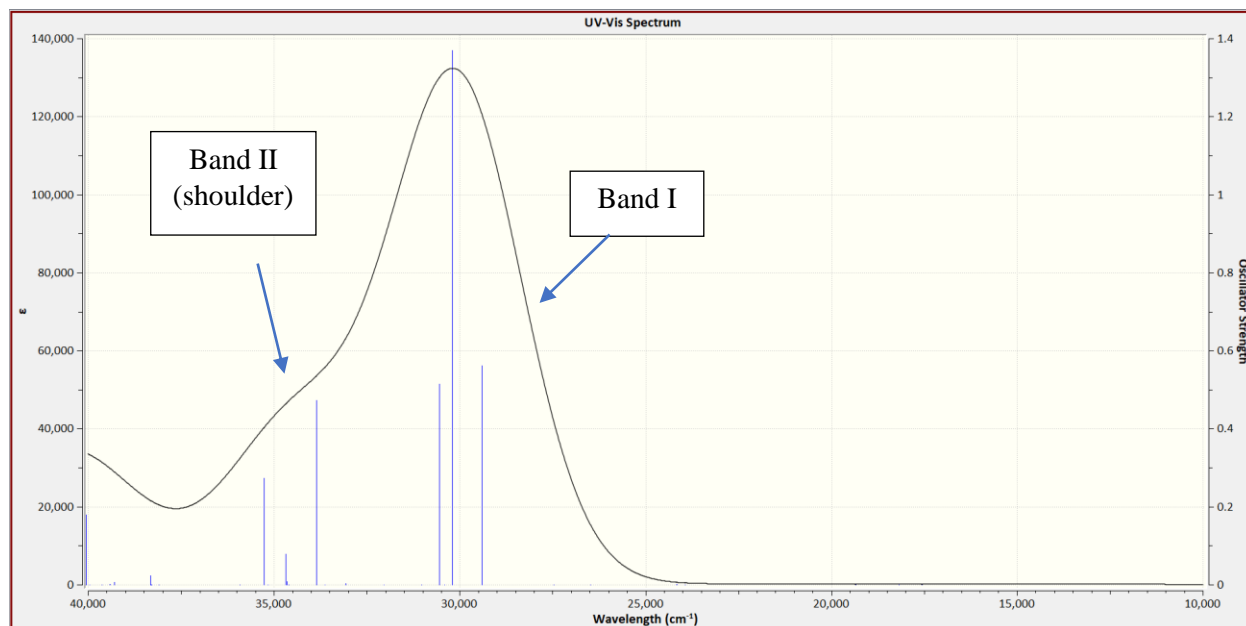
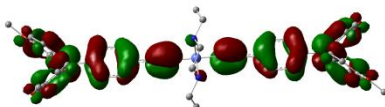
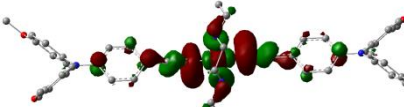
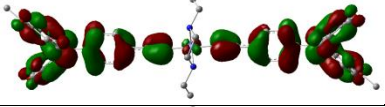
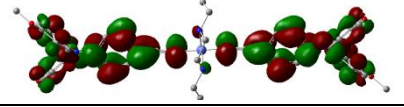
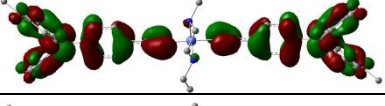
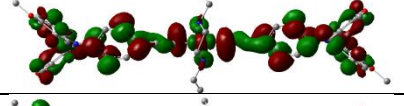
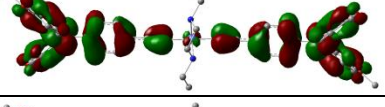
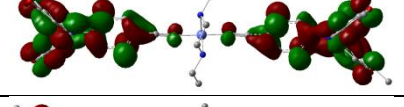
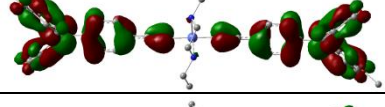
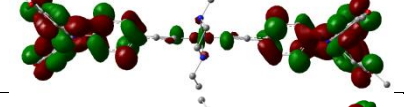
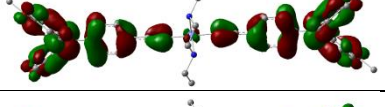
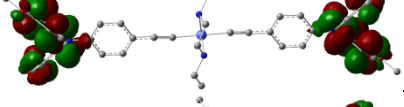
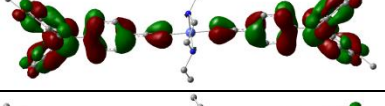
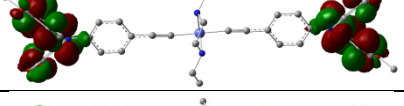
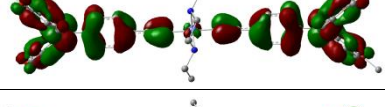
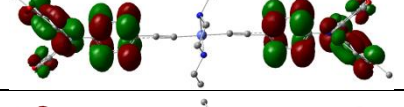
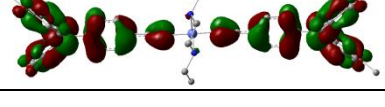
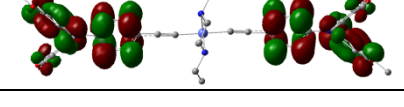


Figure S15. TD-DFT simulated UV-Vis spectrum of [3]⁺

The same issues with the simulation of the UV-Vis spectrum of compound [1]⁺ are present with that of compound [3]⁺. TD-DFT over-estimates the energies of the transitions associated with 'Band II'.

Table S6. NTOs computed for the excited states of $[3]^+$. Transitions are noted as NTO1 (hole) \rightarrow NTO2 (electron). |isovalue| = 0.025.

Excited state	$\bar{\nu}$ (cm^{-1})	Oscillator strength	NTO1	NTO2
S8	29414.4	0.562		
S9 major	30198.7	1.3693		
S9 major	30198.7	1.3693		
S11 major	30543.7	0.5154		
S11 major	30543.7	0.5154		
S17 Major	33865.0	0.4733		
S17 major	33865.0	0.4733		
S25 major	35273.4	0.2726		
S25 major	35273.4	0.2726		

Compound [3]⁺³, triplet

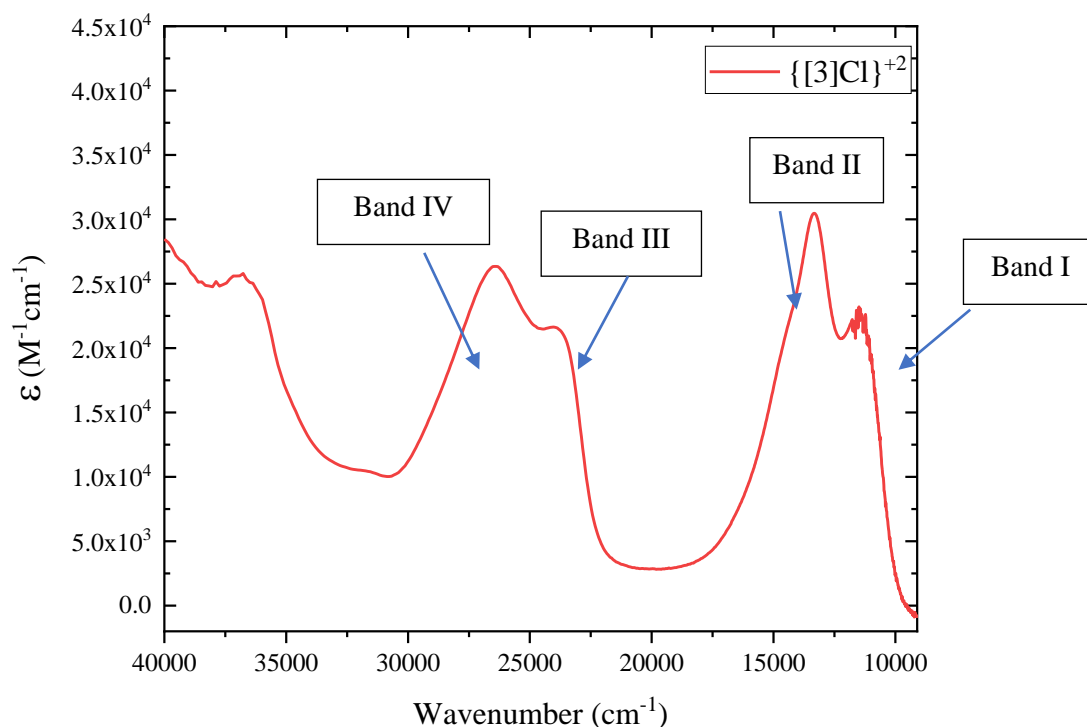


Figure S16. Experimental UV-Vis spectrum of $\{[3]Cl\}^{+2}$ in MeCN.

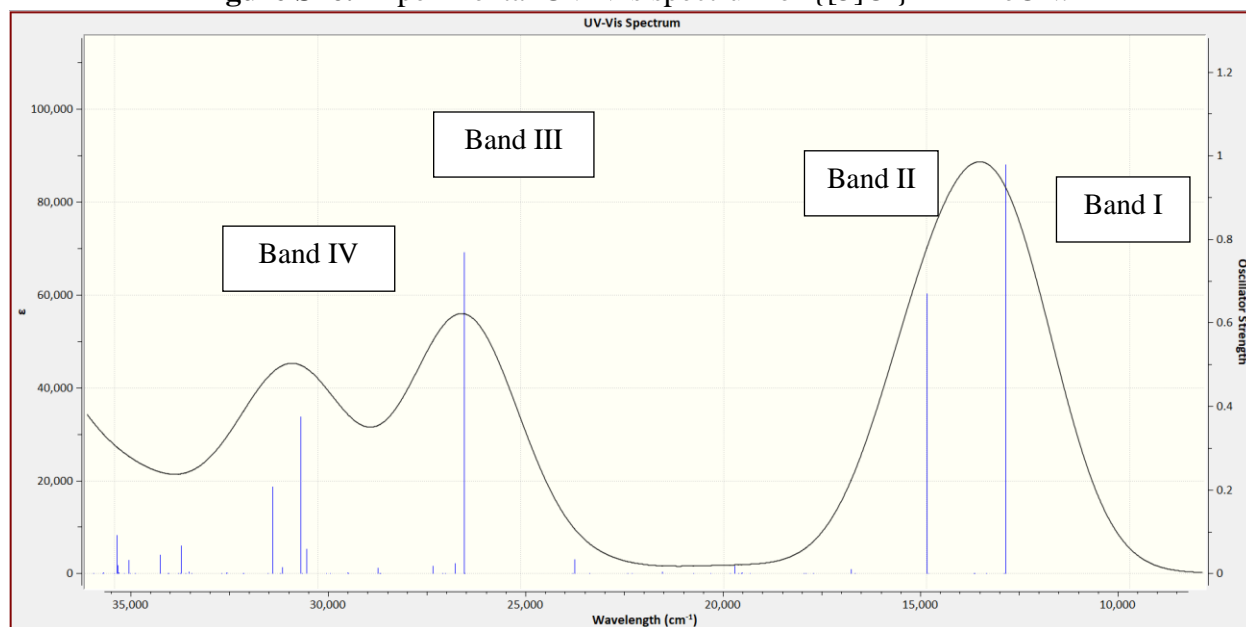
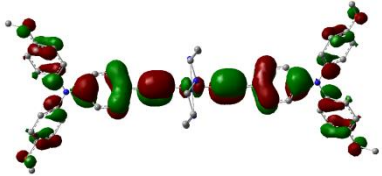
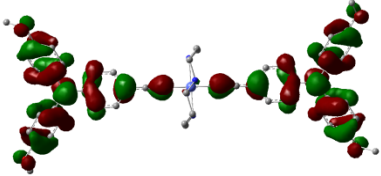
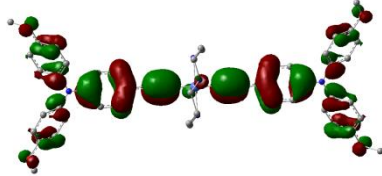
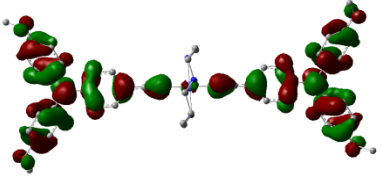
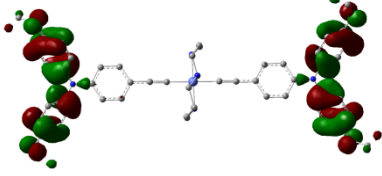
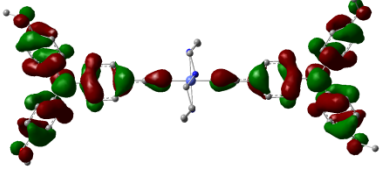
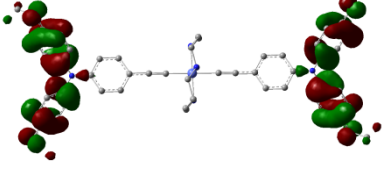
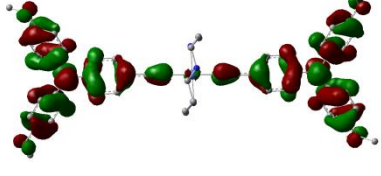
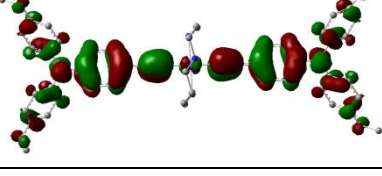
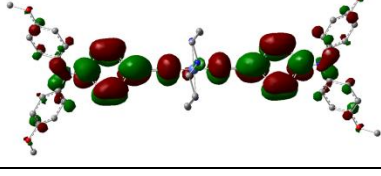
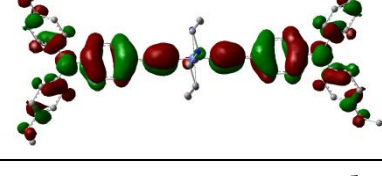
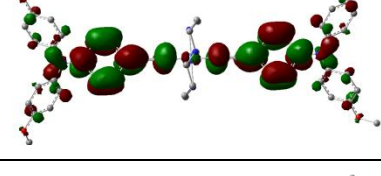
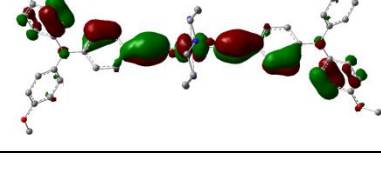
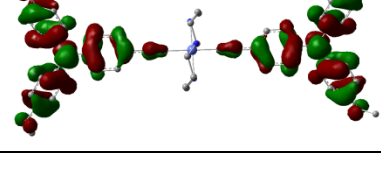
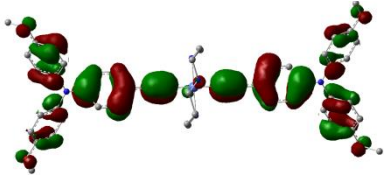
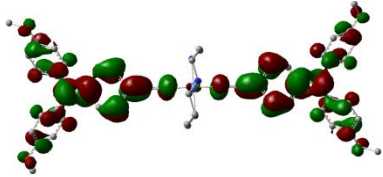
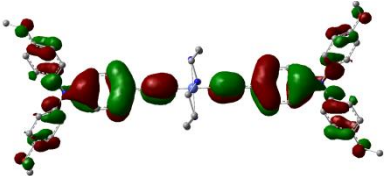
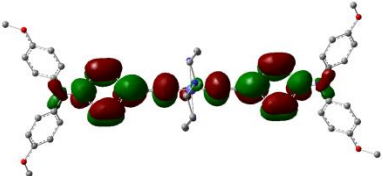
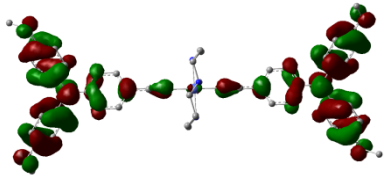
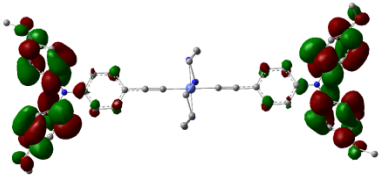
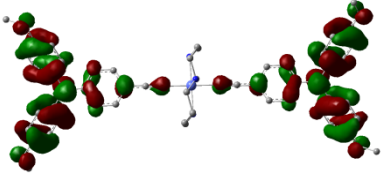
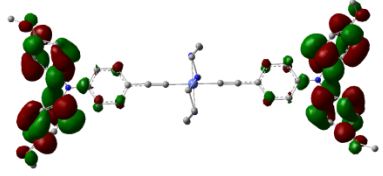
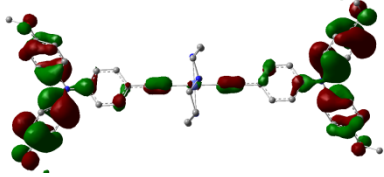
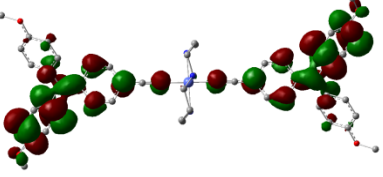
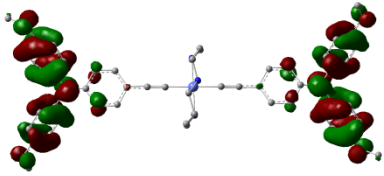
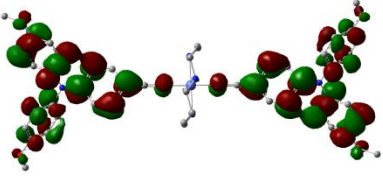
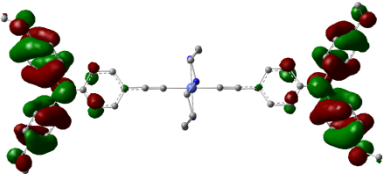
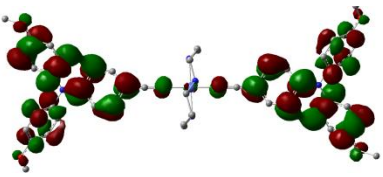
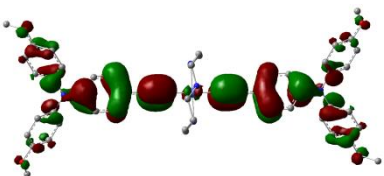
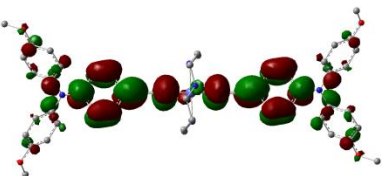


Figure S17. TD-DFT simulated UV-Vis spectrum of $[3]^{+3}$

TD-DFT fails to predict the presence of a third, shoulder band at ca. 15000 cm^{-1} . The region between 10000–20000 cm^{-1} is very similar to that of $[1]^{+2}$. The calculation also overestimates the energies associated with bands III and IV. However, it does succeed in predicting the absence of a significant absorption peak between 32000–35000 cm^{-1} .

Table S7. NTOs computed for the excited states of $[3]^{+3}$. Transitions are noted as NTO1 (hole) \rightarrow NTO2 (electron). |isovalue| = 0.025.

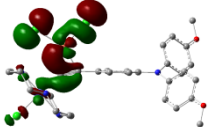
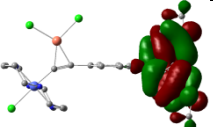
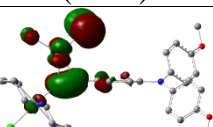
Excited state	$\bar{\nu}$ (cm^{-1})	Oscillator strength	NTO1	NTO2
T1 major	13054.5	0.9788		
T1 minor	13054.5	0.9788		
T7 Major	14987.3	0.6703		
T7 major	14987.3	0.6703		
T31 major	26394.9	0.7683		
T31 major	26394.9	0.7683		
T31 minor	26394.9	0.7683		

T31 minor	26394.9	0.7683		
T31 minor	26394.9	0.7683		
T49 major	30413.6	0.3754		
T49 major	30413.6	0.3754		
T49 minor	30413.6	0.3754		
T52 major	31111.9	0.2072		
T52 major	31111.9	0.2072		
T52 major	31111.9	0.2072		

T52 Minor	31111.9	0.2072		
T52 Minor	31111.9	0.2072		
T52 Minor	31111.9	0.2072		

Table S8. Molecular orbital diagrams plotted at $|\text{isovalue}| = 0.025$ and corresponding orbital energies (in eV) for **2a** from DFT.

LUMO+2	 (-0.68)
LUMO+1	 (-1.62)
LUMO	 (-2.01)
HOMO	 (-5.22)
HOMO-1	 (-6.44)

HOMO-2	 (-6.60)
HOMO-3	 (-6.78)
HOMO-4	 (-6.84)

References:

- (1) Sheldrick, G. M. A short history of SHELX. *Acta Crystallogr A* **2008**, *64*, 112-122.
- (2) *Gaussian 16 Rev. A.03*; Frisch, M. J.; Trucks, G. W.; Schlegel, H. B.; Scuseria, G. E.; Robb, M. A.; Cheeseman, J. R.; Scalmani, G.; Barone, V.; Petersson, G. A.; Nakatsuji, H.; Li, X.; Caricato, M.; Marenich, A. V.; Bloino, J.; Janesko, B. G.; Gomperts, R.; Mennucci, B.; Hratchian, H. P.; Ortiz, J. V.; Izmaylov, A. F.; Sonnenberg, J. L.; Williams; Ding, F.; Lipparini, F.; Egidi, F.; Goings, J.; Peng, B.; Petrone, A.; Henderson, T.; Ranasinghe, D.; Zakrzewski, V. G.; Gao, J.; Rega, N.; Zheng, G.; Liang, W.; Hada, M.; Ehara, M.; Toyota, K.; Fukuda, R.; Hasegawa, J.; Ishida, M.; Nakajima, T.; Honda, Y.; Kitao, O.; Nakai, H.; Vreven, T.; Throssell, K.; Montgomery Jr., J. A.; Peralta, J. E.; Ogliaro, F.; Bearpark, M. J.; Heyd, J. J.; Brothers, E. N.; Kudin, K. N.; Staroverov, V. N.; Keith, T. A.; Kobayashi, R.; Normand, J.; Raghavachari, K.; Rendell, A. P.; Burant, J. C.; Iyengar, S. S.; Tomasi, J.; Cossi, M.; Millam, J. M.; Klene, M.; Adamo, C.; Cammi, R.; Ochterski, J. W.; Martin, R. L.; Morokuma, K.; Farkas, O.; Foresman, J. B.; Fox, D. J.: Wallingford, CT, 2016.
- (3) Vosko, S. H.; Wilk, L.; Nusair, M. Accurate spin-dependent electron liquid correlation energies for local spin density calculations: a critical analysis. *Can. J. Phys.* **1980**, *58*, 1200-1211.
- (4) Lee, C.; Yang, W.; Parr, R. G. Development of the Colle-Salvetti correlation-energy formula into a functional of the electron density. *Phys. Rev. B* **1988**, *37*, 785-789.
- (5) Becke, A. D. Density-functional exchange-energy approximation with correct asymptotic behavior. *Phys. Rev. A* **1988**, *38*, 3098-3100.
- (6) Stephens, P. J.; Devlin, F. J.; Chabalowski, C. F.; Frisch, M. J. Ab Initio calculation of vibrational absorption and circular dichroism spectra using density functional force fields. *J. Phys. Chem.* **1994**, *98*, 11623-11627.
- (7) Yanai, T.; Tew, D. P.; Handy, N. C. A new hybrid exchange-correlation functional using the Coulomb-attenuating method (CAM-B3LYP). *Chem. Phys. Lett.* **2004**, *393*, 51-57.
- (8) Zhao, Y.; Truhlar, D. G. The M06 suite of density functionals for main group thermochemistry, thermochemical kinetics, noncovalent interactions, excited states, and transition elements: Two new functionals and systematic testing of four M06-class functionals and 12 other function. *Theor. Chem. Acc.* **2008**, *120*, 215-241.
- (9) Chai, J. D.; Head-Gordon, M. Systematic optimization of long-range corrected hybrid density functionals. *J. Chem. Phys.* **2008**, *128*, 084106.

- (10) Zhao, Y.; Truhlar, D. G. Density functional for spectroscopy: No long-range self-interaction error, good performance for Rydberg and charge-transfer states, and better performance on average than B3LYP for ground states. *J. Phys. Chem. A* **2006**, *110*, 13126-13130.
- (11) Weigend, F.; Ahlrichs, R. Balanced basis sets of split valence, triple zeta valence and quadruple zeta valence quality for H to Rn: Design and assessment of accuracy. *Phys. Chem. Chem. Phys.* **2005**, *7*, 3297-3305.
- (12) Francl, M. M.; Pietro, W. J.; Hehre, W. J.; Binkley, J. S.; Gordon, M. S.; DeFrees, D. J.; Pople, J. A. Self-consistent molecular orbital methods. XXIII. A polarization-type basis set for second-row elements. *J. Chem. Phys.* **1982**, *77*, 3654-3665.
- (13) Hariharan, P. C.; Pople, J. A. The influence of polarization functions on molecular orbital hydrogenation energies. *Theor. Chim. Acta* **1973**, *28*, 213-222.
- (14) Cossi, M.; Rega, N.; Scalmani, G.; Barone, V. Energies, structures, and electronic properties of molecules in solution with the C-PCM solvation model. *J. Comput. Chem.* **2003**, *2*, 669-681.
- (15) Barone, V.; Cossi, M. Quantum calculation of molecular energies and energy gradients in solution by a conductor solvent model. *J. Phys. Chem. A* **1998**, *102*, 1995-2001.
- (16) Grimme, S.; Antony, J.; Ehrlich, S.; Krieg, H. A consistent and accurate ab initio parametrization of density functional dispersion correction (DFT-D) for the 94 elements H-Pu. *J. Chem. Phys.* **2010**, *132*, 154104.
- (17) Zhang, M. X.; Zhang, J.; Yin, J.; Hartl, F.; Liu, S. H. Anodic electrochemistry of mono- and dinuclear aminophenylferrocene and diphenylaminoferrocene complexes. *Dalton Trans.* **2018**, *47*, 6112-6123.
- (18) Hirata, S.; Head-Gordon, M. Time-dependent density functional theory within the Tamm-Dancoff approximation. *Chem. Phys. Lett.* **1999**, *314*, 291-299.
- (19) Martin, R. L. Natural Transition Orbitals. *J. Chem. Phys.* **2003**, *118*, 4775-4777.